ACS APPLIED MATERIALS & INTERFACES

Research Article

www.acsami.org

Monitoring Dopamine Quinone-Induced Dopaminergic Neurotoxicity Using Dopamine Functionalized Quantum Dots

Wei Ma, Hui-Ting Liu, and Yi-Tao Long*

Key Laboratory for Advanced Materials & Institute of Fine Chemicals, East China University of Science and Technology, Shanghai, 200237, P. R. China

Supporting Information

ABSTRACT: Dopamine (DA) quinone-induced dopaminergic neurotoxicity is known to occur due to the interaction between DA quinone and cysteine (Cys) residue, and it may play an important a role in pathological processes associated with neurodegeneration. In this study, we monitored the interaction process of DA to form DA quinone and the subsequent Cys residue using dopamine functionalized quantum dots (QDs). The fluorescence (FL) of the QD bioconjugates changes as a function of the structure transformation during the interaction process, providing a potential FL tool for monitoring dopaminergic neurotoxicity.

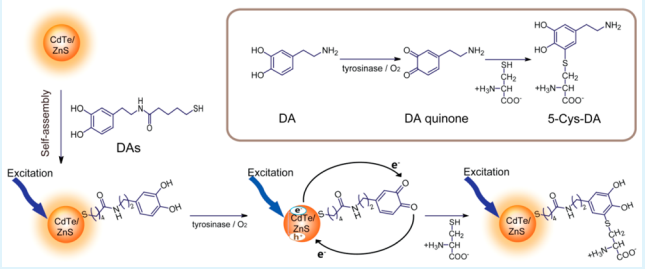

KEYWORDS: *dopaminergic neurotoxicity, quantum dots, dopamine quinone, cysteine residue, fluorescence*

INTRODUCTION

Dopamine (DA) is a central nervous system neurotransmitter that performs various functions in the brain. Under oxidative stress, DA can readily oxidize to form DA quinone catalyzed by enzyme tyrosinase/O_2, and it participates in nucleophilic addition with sulfhydryl groups on free cysteine (Cys), glutathione (GSH), or Cys residue found in proteins.[1,2] The interaction between the Cys residue and DA quinone results in the in vivo and in vitro formation of 5-Cys-DA, as shown in the inset of Figure 1.

The Cys residue plays vital roles in biological protection mechanisms and physiological function. However, DA inactivation modification between the Cys residue and DA quinone may scavenge the thiol protein, inhibit protein function, and disturb mitochondrial function because the sulfhydryl group on Cys is often located at the active site of functional proteins.[3] In addition, this modification decreases the endogenous level of Cys residues, which is critical for maintaining the dynamic redox balance of cell.[3] Previous results have suggested that disturbance of Cys residue homeostasis may lead to or result from oxidative stress in cells, contributing to early mitochondrial dysfunction and resulting in neurodegenerative pathogenesis.[4] For example, 5-Cys-DA has been found in cerebrospinal fluid of individuals with Parkinson's disease (PD)[5,6] and may contribute to PD pathogenesis.[7] Therefore, DA quinone formation may induce dopaminergic neurotoxicity and play a role in pathological processes associated with neurodegeneration.[8] Studies of the interactions of DA to form DA quinone and the subsequent Cys residue as dopaminergic neuron-specific oxidative stress may provide a potential path for monitoring DA quinone-induced neurotoxicity. Therefore, it is of considerable significance to investigate the nature of this interaction process in physiology and pathology.

Semiconductor quantum dots (QDs) are light-emitting nanoparticles that exhibit superior optical and photophysical properties. The biorecognition or biocatalytic reactions have been followed by fluorescence (FL) resonance energy transfer or electron transfer processes stimulated by excited QDs.[9] Redox-active biomolecule functionalized QDs have generated much interest in recent years.[10−14] For example, QD−DA−peptide bioconjugates can function as in vitro and intracellular pH sensors.[15,16] NADH:ubiquinone oxidoreductase detection and reactive oxygen species (ROS) sensing has been achieved by ubiquinone-QD bioconjugates via a redox mechanism.[17,18] Coupling QDs with cytochrome c is suitable for FL imaging of superoxide radicals.[19] However, few examples demonstrate the application of the photophysical properties of QDs for monitoring intraneural reactions using FL probe. In addition, how to explore the nanoparticles as valuable monitoring tools for neurotransmitter inactivation progress is lacking at the present time. In this study, the photophysical properties of semiconductor QDs were used to monitor the redox process of *N*-(3,4-dihydroxyphenethyl)-5-mercaptopentanamide (**DAs**) and the formation of 5-Cys-**DAs** by mimicking the interaction process involving the oxidation of DA to form DA quinone, which binds covalently to nucleophilic sulfhydryl groups on Cys residues. The interaction process leads to structure transformation between DA quinone and catechol, inducing a FL change in the functionalized QD bioconjugates (Figure 1).

Received: April 9, 2015
Accepted: June 12, 2015
Published: June 12, 2015

DOI: 10.1021/acsami.5b03044
ACS Appl. Mater. Interfaces 2015, 7, 14352−14358

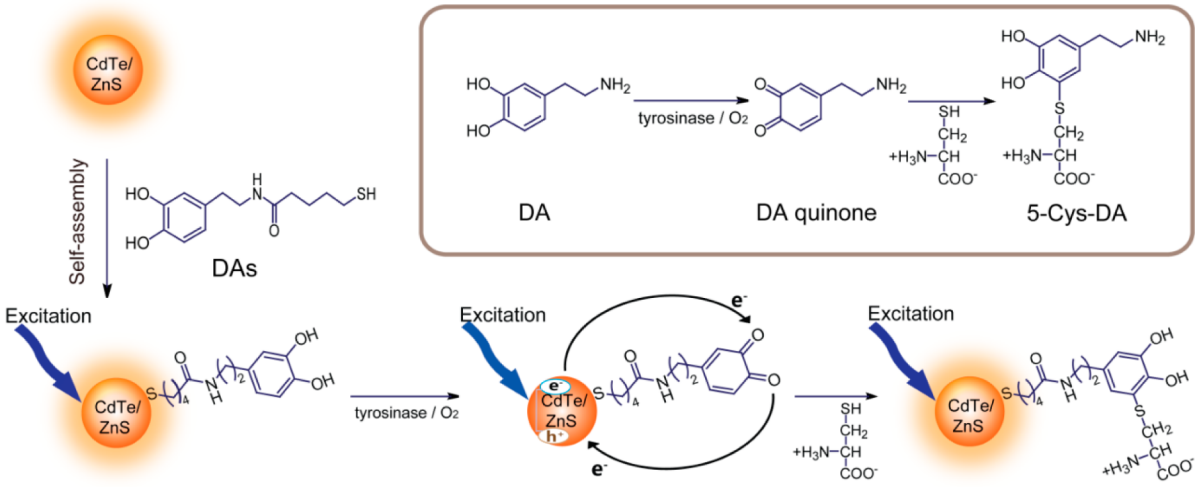

Figure 1. Schematic diagram of the self-assembly and FL quenching/recovery characteristics of *N*-(3,4-dihydroxyphenethyl)-5-mercaptopentanamide (**DAs**) functionalized CdTe/ZnS QDs. (Inset) Schematic representation of the oxidation of DA and the irreversible interaction between the Cys residue and DA quinone.

Several lines of evidence suggest that this interaction process is related to dopaminergic neurotoxicity. Therefore, the FL changes in this proposed system provide a useful FL platform for monitoring neurotransmitter modification.

EXPERIMENTAL SECTION

Synthesis of CdTe/ZnS QDs. In a three-necked flask (250 mL) equipped with a reflux condenser, septa, and valves, $CdCl_2 \cdot 2.5H_2O$ (0.2987 g, 1.31 mmol) was dissolved in degassed water (98.0 mL). Mercaptopropionic acid (MPA; 0.118 mL, 1.7 mmol) was added, and the pH of the solution was adjusted to 11.2 with an aqueous NaOH solution (1 M) followed by stirring under bubbling N_2 at room temperature for 30 min. Then, the clear supernatant solution containing NaHTe was added under N_2, and the Cd/MPA/Te molar ratio was set to 1.2:1.3:0.54 with an initial Cd^{2+} concentration of 13.05 mM.[20] The mixture consisting of the precursor materials turned from colorless to dark orange and was then refluxed to allow the QDs to grow. A solution of $ZnSO_4$ (1.25 mM) in MPA (40 mL) was quickly injected into the prepared CdTe solution (15 mL), and Na_2S was simultaneously added with vigorous stirring, which resulted in immediate nucleation and growth of the nanoparticles. Then, the pH was adjusted to 11.2 by adding l M NaOH ($Zn^{2+}/Cd^{2+}/S^{2-}$/MPA = 1:0.2:0.4:2.4). The precipitates were centrifuged, sequentially washed with water and acetone, and dried with N_2. For the preparation of the nanocrystal thin-film, the resulting powders were ultrasonically dispersed in ethanol and then filtered to obtain a colloidal solution consisting of CdTe/ZnS QDs, which was maintained in a refrigerator at 4−8 °C.

Preparation of Functionalized CdTe/ZnS QDs. The prepared CdTe/ZnS QDs (λ_{em} = 596 nm) were incubated with different amounts of 0.2 mM **DAs** at room temperature and shaken vigorously under the protection of N_2 for 2 h. Then, acetone was added with a volume ratio of 1:1 into the mixture, and the suspension was centrifuged at 7840 rpm for 20 min. The clear supernatant was discarded, and a pellet of **DAs**-CdTe/ZnS QDs nanocrystals was obtained.[21] The same amount of acetone was added to the resulting nanocrystals. Then, the suspension was centrifuged, and the clear supernatant was discarded. This procedure was repeated three times to yield the purified functionalized QD bioconjugates. The obtained crystals were maintained in a refrigerator prior to testing. Because dopamine can be easily oxidized by molecular O_2, especially in high pH solutions, the pH of the reaction solution was maintained at 6.5 with degassing for 5−10 min to prevent dopamine autoxidation and maintained the FL stability of the QD bioconjugates. We employed a relative optical method to determine the FL quantum yield of the QD bioconjugates.[22] The quantum yield at room temperature was estimated according to the maximum emission wavelengths of the QD bioconjugates. Rhodamine 6G in ethanol was chosen as the reference standard (QY 95%). All optical measurements were performed at room temperature under ambient conditions.

Cell Culture, Cellular Imaging, and Cytotoxicity. Human cervical carcinoma cells (HeLa line) were cultured in minimal essential medium (MEM; WelGene Inc., Seoul, Korea) supplemented with 10% fetal bovine serum (FBS; WelGene), penicillin (100 units/mL), and streptomycin (100 μg/mL). Two days prior to imaging, the cells were passed and plated on glass-bottomed dishes (MatTek). The cells were maintained in a 5% humidified CO_2 air environment at 37 °C. The HeLa cells were plated into a 24-well culture plate (200−300 cells per well) and allowed to adhere for 24 h prior to treatment. The cells were incubated with **DAs**-functionalized CdTe/ZnS QDs or pretreated with different concentrations of NEM for 30 min followed by incubation with **DAs** quinone-QDs for 12 h. The cells were fixed with a 4% methanal solution at room temperature for 20 min followed by washing with PBS three times prior to imaging. All of the background parameters (i.e., laser intensity, exposure time, and objective lens) were held constant when the different confocal images were captured. The excitation wavelength of the **DAs** quinone-QDs was 540 nm. The cytotoxicity assay was performed using the MTT (3-(4,5-dimethylthiazol-2-yl)-2,5-diphenyltetrazolium bromide) method. The HeLa cells were placed in 96-well culture plates (10^4 cells per well) and allowed to attach for 12 h prior to treatment. The cells were treated with **DAs** quinone-QDs ranging from 0.05 to 5 nM. The cell viability was evaluated using the MTT assay after 24 h of treatment. The optical density (OD) in the control and sample-treated wells was measured using an automated microplate reader (Multiskan Ex, Lab systems, Finland) at a test wavelength of 450 nm. The cytotoxicity of the functionalized QD bioconjugates is expressed as IC_{50} (concentration of 50% cytotoxicity, which was extrapolated from linear regression analysis of the experimental data).

Determination of Intracellular Cys Residue Content. The number of thiol groups was determined using modified a Ellman method. The HeLa cells were plated into a 6-well culture plate (200−300 cells per well) and allowed to attach for 24 h. After 12 h of incubation with the indicated concentrations of NEM in culture medium, the cells were washed twice in ice-cold PBS and collected by scraping. The cell extracts were collected using two rapid freezing and thawing cycles at the temperature liquid nitrogen and 37 °C. The samples were centrifuged at 10 000*g* for 5 min at 4 °C. The supernates were mixed with 0.25 M Tris-HCl (pH = 8.3) to determine the Cys residue content using 5,5-dithiobis(2-nitrobenzoic acid) (DTNB; Sigma, St. Louis, MO). Standard curves were made using different

DOI: 10.1021/acsami.5b03044
ACS Appl. Mater. Interfaces 2015, 7, 14352−14358

known concentrations of Cys residue. The concentration of Cys residue in a sample solution was determined using the OD measurement at an absorbance of 412 nm.

RESULTS AND DISCUSSION

The DA-functionalized QDs were prepared via the following steps: (1) 596 nm emitting mercaptopropionic acid (MPA)-capped CdTe/ZnS QDs and a redox-active DA thiol derivative (*N*-(3, 4-dihydroxyphenethyl)-5-mercaptopentanamide (**DAs**)) as a surface-capping ligand were designed and synthesized. (2) The ligand molecule (**DAs**) was self-assembled onto the surface of the QDs. As shown in Figure 2a, comparative studies of the

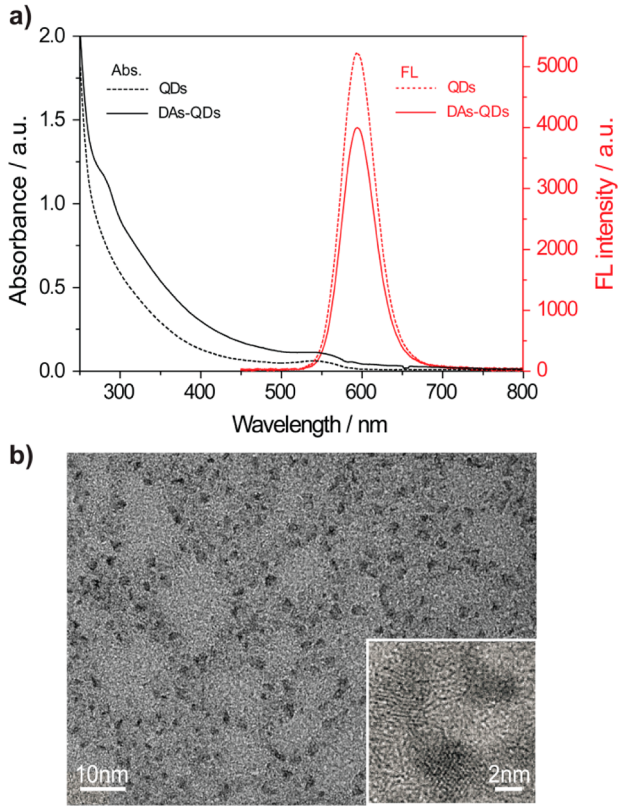

Figure 2. (a) Representative (red) FL spectra and (black) UV–vis spectra collected from (dotted line) bare QDs and (solid line) **DAs**-QDs in a PBS buffer at a pH of 6.5. (b) TEM of **DAs**-QDs and (inset) a magnified area.

UV–vis spectra and FL spectra for bare QDs and **DAs**-functionalized QD bioconjugates indicate self-assembling of **DAs** on the QDs surfaces. The high-resolution transmission electron microscopy (TEM) results indicated that the nanoparticle size of the QD bioconjugates was approximately 4 nm, and the particles were dispersed homogeneously (Figure 2b). Dynamic light scattering (DLS) of the bare CdTe/ZnS QDs in aqueous solution indicated that the QDs have a narrow size distribution with an average size of 3.6 nm (Figure S4, Supporting Information, black line). However, the **DAs**-QDs bioconjugates were slightly larger with an average size of 4.1 nm (Figure S4, Supporting Information, red line), which is consistent with the coating of sulfhydryl compounds onto the surface of the QDs.[23] New peaks that appeared in the ^{1}H NMR spectrum of the purified **DAs** functionalized QDs correspond to the assembled **DAs** ligand, which also confirms the successful attachment of **DAs** to the QDs (Figure S5, Supporting Information). In addition, high-performance liquid chromatography was performed on a 30 cm long size-exclusion column. Representative size exclusion chromatography (SEC) results indicate that the retention time of the **DAs**-functionalized QDs (Figure S6, Supporting Information, red line) decreased compared to that of bare CdTe/ZnS QDs (Figure S6, Supporting Information, black line). As expected for a size exclusion process, the larger particles (**DAs** functionalized QDs) elute first, indicating that **DAs** form a stable coating on the surface of the CdTe/ZnS QDs. Approximately 24 **DAs** molecules per QD was chosen as the optimal ratio based in the spectra for the QDs self-assembled with increasing ratios of **DAs** (Figure S7, Supporting Information). The **DAs** quinone on the surface of the QD bioconjugates is generated from the enzymatic oxidation of **DAs** by tyrosinase/O_2, resulting in FL quenching. To achieve the maximum activity of tyrosinase, we performed the reaction process in PBS buffer for 10 min at a pH 6.5 and 25 °C. As shown in Figure 3, upon addition of a 3-

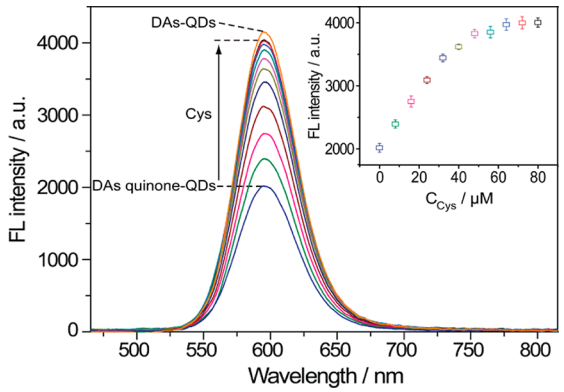

Figure 3. Representative FL spectra of the (top orange line) **DAs**-QDs, **DAs**-QDs upon tyrosinase addition in the presence of O_2 to obtain (bottom blue line **DAs** quinone-QDs), and **DAs** quinone-QDs system with varying Cys concentrations from 0 to 80 μM. (Inset) Relationship between the FL of the **DAs** quinone-QDs and increasing concentrations of Cys.

fold maximum tyrosinase (3.6 U) in the presence of O_2, the FL intensity of the functionalized QDs was significantly quenched, as expected. In contrast, additional excess of tyrosinase did not significantly affect the FL of the bare CdTe/ZnS QDs (≤10% quenching). After the **DAs**-QDs were oxidized by tyrosinase/O_2, the **DAs** quinone product functioned as an excellent electron acceptor molecule that was efficient at hole trapping of QDs and resulted in FL quenching.[15,16,18] According to the calculation, quantum yields of the **DAs**-CdTe/ZnS QDs and **DAs** quinone-CdTe/ZnS QDs were 81 and 52%, respectively (Figure S8, Supporting Information), enabling the use of following detection with high sensitivity.

To confirm the interaction between DA quinone and the Cys residue with different FL properties on **DAs** quinone functionalized QDs, we measured the FL intensity of functionalized QDs at different concentrations of Cys in PBS buffer at a pH 6.5 and 25 °C. As shown in Figure 3, the FL intensity of the **DAs** quinone-QD bioconjugates gradually recovered upon addition of increasing amounts of Cys. Approximately 96% of the FL was recovered after addition of 80 μM Cys. The inset in Figure 3 shows the recovery of the FL intensity as a function of the Cys concentration, and saturation was reached after approximately 65 μM. It is noteworthy that

DOI: 10.1021/acsami.5b03044
ACS Appl. Mater. Interfaces 2015, 7, 14352–14358

the formation of 5-Cys-**DAs** containing catechol on the functionalized CdTe/ZnS QDs resulted in significant FL recovery. Here, the photoexcited QD bioconjugates decay radiatively to the ground state because the 5-Cys-**DAs** ligands can act as poor electron acceptor/donors. This, in turn, will result in FL recovery compared to that of **DAs** quinone functionalized QDs, impairing the electron transfer from QDs to quinone. We demonstrated that the Cys-induced reaction with **DAs** quinone-QDs generated the catechol product on the surface of the QDs using differential UV−vis absorption (Figure S9, Supporting Information) and the characteristic band in the Fourier transform infrared spectroscopy (FTIR) spectrum (Figure S10, Supporting Information).[24] The surface-enhanced Raman scattering (SERS) spectra (Figure S11, Supporting Information) of **DAs** obtained upon interaction with tyrosinase/O_2 followed by Cys also confirmed the evolution of **DAs** to the fully oxidized state and then its return to its Cys-**DAs** form.[25,26] Mass spectrometric analysis was also performed to examine the reactions of **DAs** quinone with Cys (Figure S12, Supporting Information). The reaction mixtures of **DAs** quinone with Cys exhibited a new peak with m/z = 383, corresponding to the deprotonated addition product (i.e., **DAs**-Cys conjugates). The new peaks were not detected when **DAs** was incubated alone followed by tyrosinase-catalyzed oxidation and barely detected in the absence of tyrosinase under the same conditions. This result confirmed the formation of the 5-**DAs**-Cys adduct as the major product when Cys was added to the **DAs**-quinone-functionalized QDs. The changes in the UV−vis spectra, FTIR spectra, SERS peaks, and mass spectrometric analysis are consistent with the structural transition of quinone and catechol upon the interaction. These studies suggest that the **DAs**-quinone-functionalized QD system could be used to track the interaction process between DA quinone and the Cys residue. Because dopamine can be easily oxidized by oxygen, the stability of the **DAs**-CdTe/ZnS QDs and **DAs** quinone−CdTe/ZnS QDs were investigated in PBS buffer at a pH of 6.5 and room temperature (25 °C). The **DAs**-functionalized QDs produced a negligible change in the PL intensity (Figure S13A, Supporting Information), indicating that **DA** remained in the reduced state under the experimental conditions for at least 10 min. Similarly, the QDs with **DAs** quinone barely led to any PL signal variation (Figure S13B, Supporting Information), which indicates the stability of our system for monitoring the interaction process of DA to form DA quinone and the subsequent Cys residue using **DAs**-QDs.

To investigate the possible interferences of this FL monitor, we measured the FL changes of the **DAs** quinone-QDs in the presence of other representative thiol compounds, such as 4-methoxy-α-toluenethiol, 11-mercaptoundecanoic acid, (4-sulfanylphenyl) boronic acid, 4-mercaptobenzoicacid, hexyl mercaptan, 4-aminothiophenol, *n*-octadecylmercaptan, *n*-octylmercaptan, ethylenemercaptan, and 2-mercaptoethanol (Figure 4). Remarkably, no obvious FL recovery of the **DAs** quinone-QDs was observed at the same concentration (80 μM) upon introduction of these thiol compounds. Moreover, the FL changes of the **DAs** quinone-QDs with other reducing agents, such as NADH and ascorbic acid, were also investigated. No FL recovery response was detected for the **DAs** quinone-QD bioconjugates (Figure S14, Supporting Information). The proposed QD bioconjugates exhibit unique discriminative properties for thiol compounds containing Cys residues. These results demonstrate that the FL intensity recovery arises from the specific interaction of the Cys residue and **DAs**

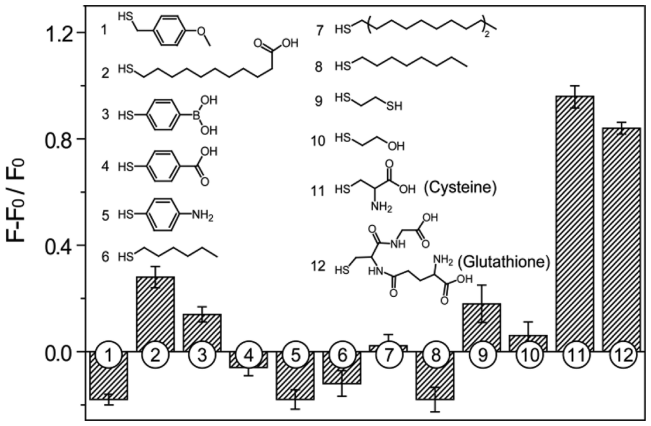

Figure 4. FL recovery intensity of the **DAs** quinone-QDs in the presence of different thiol compounds.

quinone rather than Cys displacing the **DAs** ligands on the surface of the QDs.[12] In addition, the same amount of Cys residue compounds did not affect the FL of bare QDs, **DAs**-QDs, and ubiquinone-functionalized QDs (**Q_1S**-QDs), which further confirmed that the Cys-induced FL recovery of the **DAs** quinone-QDs was not a ligand displacement process (Figure S15, Supporting Information). Only the presence of Cys residues (Cys or GSH) induced rapid FL recovery of the **DAs** quinone functionalized QDs (Figure S16, Supporting Information), confirming the specific coupling of Cys and **DAs** quinone in this system.

The FL response to the protein containing Cys residues using this probe was further investigated. Bovine serum albumin (BSA) is major soluble thiol protein constituent in the circulatory system. BSA plays a dominant role in the transport and disposition of endogenous and exogenous compounds present in blood.[27,28] Therefore, BSA was selected as our protein model. The FL of the bare QDs was not affected by the addition of BSA. However, the addition of increasing amounts of BSA to the solution containing the **DAs** quinone-QDs resulted in FL intensity recovery, as shown in Figure 5. In BSA binding to the **DAs** quinone ligands, the Cys residues induce the formation of Cys-**DAs** including a catechol

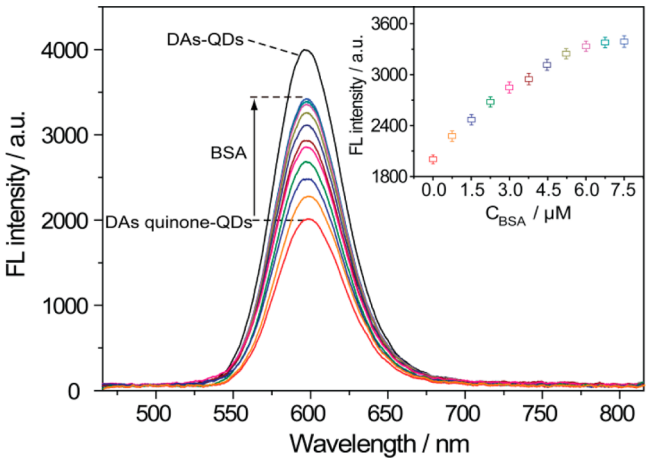

Figure 5. Representative FL spectra of **DAs**-QDs, **DAs** quinone-QDs system with BSA concentrations varying from (top to bottom) 0 to 7.5 μM. (Inset) Relationship between the FL of **DAs** quinone-QDs and increasing concentrations of BSA.

DOI: 10.1021/acsami.5b03044
ACS Appl. Mater. Interfaces 2015, 7, 14352−14358

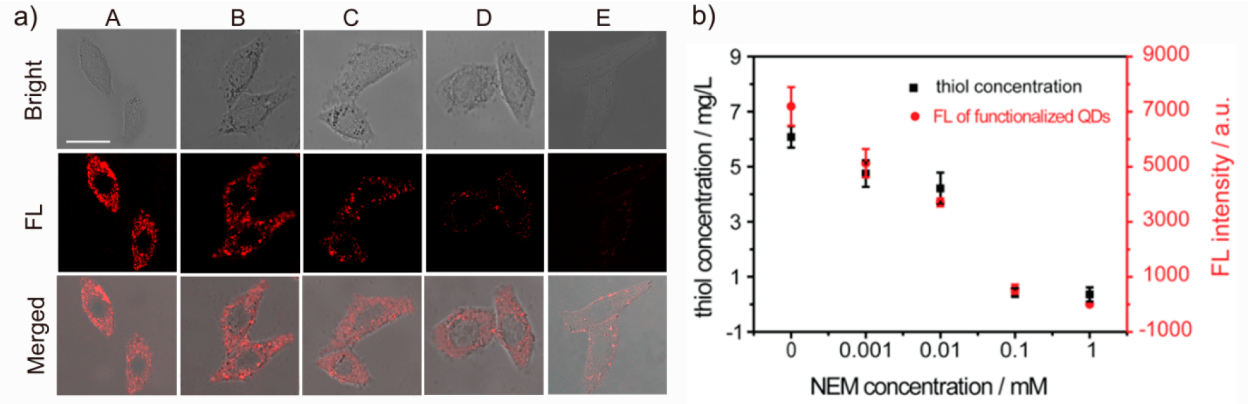

Figure 6. (a) Bright field images, FL micrographs and merged images of **DAs** quinone-QDs collected from (A) human HeLa cells and HeLa cells pretreated with (B) 0.001 mM, (C) 0.01 mM, (D) 0.1 mM, and (E) 1 mM NEM. Scale bar = 25 μm. (b) Spots of thiol concentration derived from (black) the Ellman method shown along with (red) the FL intensity as a function of the NEM concentration. Good agreement between the thiol concentration and the FL intensity was observed.

structure, which alters the FL of the QD bioconjugates. The inset in Figure 5 shows that the FL intensity increased by 71% after the addition of the 7.5 μM BSA and achieved saturation, and this result is less than the FL intensity recovery induced by Cys or GSH. The different response was most likely due to the different spatial structure of the two amino acid Cys.[29] However, BSA exhibited a similar recovery effect on the FL of QD bioconjugates. We also investigated the binding of **DAs**-quinone-functionalized QDs to non-Cys-containing proteins as a negative control. As shown in Figure S17 (Supporting Information), **DAs**-quinone-functionalized QDs resulted in almost no PL recovery with non-Cys-containing proteins (horse myoglobin and bovine carbonic anhydrase), indicating that the FL intensity recovery arises from the specific interaction of **DAs** quinone and the Cys residue of the thiol protein. All results indicated that the **DAs** quinone-QDs are a potent tool for investigating proteins with Cys residue.

On the basis of these results, the **DAs** quinone-QDs may be employed as a biocompatible FL platform for monitoring dopaminergic neurotoxicity by tracking the interaction between Cys residue and **DAs** quinone. We developed a model to image the intracellular interaction progress using human HeLa cells labeled with **DAs** quinone-QDs by high-resolution confocal microscopy. The Cys level decreased in the HeLa cells after 30 min of treatment with 0.001, 0.01, 0.1, and 1 mM N-ethylmaleimide (NEM), which is a well-known thiol-inactivation agent.[30] The Ellman method has been used to quantify the Cys residue level in the cell region.[31,32] For cells no treated with NEM, the FL of the QD bioconjugates is strikingly bright with a spotty stain appearance (Figure 6a-A). For the cells incubated with increasing concentrations of NEM, the QD labeling produces a moderate FL (Figure 6a-B). A further observation revealed that the FL of the QD bioconjugates became weaker on cells with lower Cys residues level. This result suggests that reducing the Cys level results in decreased PL recovery of the **DAs** quinone-QDs (Figure 6a-C,D). At the maximum NEM concentration under the cellular incubation conditions, the QD labeling throughout the cells exhibited almost no FL under identical conditions (Figure 6a-E). The decrease in the QD FL was correlated with the thiol deficiency of the Cys residues. The FL intensity was superimposed on the concentration of the cellular thiol level, and the FL response as a function of the NEM concentration was consistent with the cellular thiol level (Figure 6b). This result implies that the **DAs** quinone-QDs can quantitatively monitor intracellular thiol levels of Cys residues. As shown in Figure 6a, FL labeling was primarily localized in the nonorganelle cytoplasmic areas and the perinuclear region. The delivery of **DAs** quinone functionalized QDs to the HeLa cells is predominantly based on specific uptake following receptor−mediator endocytosis.[33,34] When incubated with HeLa cells, the extracellular QDs are recognized by the dopamine receptor due to specific binding between quinone and the cysteine sulfhydryl of the receptor.[35−37] In addition, we also investigated the cytotoxicity of **DAs** quinone-QD labeled HeLa cells using the MTT assay. It is important to note that after the addition of the **DAs** quinone-QDs, cell viability was more than 80% at concentrations ranging from 0.05 to 5 nM (Figure S18, Supporting Information). These experimental results suggest that our developed **DAs**-QDs system is cell-permeable and biocompatible with exciting possibilities for monitoring DA quinone-induced dopaminergic neurotoxicity by mimicking the neurotransmitter inactivation process.

CONCLUSION

In summary, we have developed a novel FL platform for monitoring the interaction process of DA to form DA quinone and the subsequent Cys residue using dopamine functionalized QDs. This type of approach is the first report to track the redox process of **DAs** and the formation of 5-Cys-**DAs** by mimicking the inactivation process of the DA neurotransmitter based on the FL changes of the QD bioconjugates as a function of the structure transformation during the interaction process. Due to the relationship between oxidative stress and neurodegenerative pathogenesis, this FL tool may eventually lead to diagnosis and monitoring of neurodegenerative diseases in their early stage by relying on the unique photophysical properties of QDs.

ASSOCIATED CONTENT

Supporting Information

Experiment details. The Supporting Information is available free of charge on the ACS Publications website at DOI: 10.1021/acsami.5b03044.

DOI: 10.1021/acsami.5b03044
ACS Appl. Mater. Interfaces 2015, 7, 14352−14358

AUTHOR INFORMATION

Corresponding Author

*Yi-Tao Long: Fax: 86-21-64252339, E-mail: ytlong@ecust.edu.cn.

Author Contributions

The manuscript was written through contributions of all authors. All authors have given approval to the final version of the manuscript.

Notes

The authors declare no competing financial interest.

ACKNOWLEDGMENTS

This research was supported by the 973 Program (2014CB748500 and 2013CB733700), the National Natural Science Foundation of China (21125522, 21305045, 21327807), and the Fundamental Research Funds for the Central Universities (WJ1313004).

REFERENCES

(1) Hastings, T. G.; Lewis, D. A.; Zigmond, M. J. Role of Oxidation in the Neurotoxic Effects of Intrastriatal Dopamine Injections. *Proc. Natl. Acad. Sci. U.S.A.* **1996**, *93*, 1956−1961.

(2) Laar, V. V.; Dukes, A. A.; Cascio, M.; Hastings, T. G. Proteomic Analysis of Rat Brain Mitochondria Following Exposure to Dopamine Quinone: Implications for Parkinson Disease. *Neurobiol. Dis.* **2008**, *29*, 477−489.

(3) Miyazaki, I.; Asanuma, M. Approaches to Prevent Dopamine Quinone-Induced Neurotoxicity. *Neurochem. Res.* **2009**, *34*, 698−706.

(4) Finkel, T. Oxidant Signals and Oxidative Stress. *Curr. Opin. Cell. Biol.* **2003**, *5*, 247−254.

(5) Lin, M. T.; Beal, M. F. Mitochondrial Dysfunction and Oxidative Stress in Neurodegenerative Diseases. *Nature* **2006**, *43*, 787−795.

(6) Shen, X. M.; Xia, B.; Wrona, M. Z.; Dryhurst, G. Synthesis, Redox Properties, in Vivo Formation, and Neurobehavioral Effects of N-Acetylcysteinyl Conjugates of Dopamine: Possible Metabolites of Relevance to Parkinson's Disease. *Chem. Res. Toxicol.* **1996**, *9* (7), 1117−1126.

(7) Höglinger, G. U.; Rizk, P.; Muriel, M. P.; Duyckaerts, C.; Oertel, W. H.; Caille, I.; Hirsch, E. C. Dopamine Depletion Impairs Precursor Cell Proliferation in Parkinson Disease. *Nat. Neuros.* **2004**, *7* (7), 726−735.

(8) Arancibia, S.; Martinez, C.; Barenque, L.; Lendrick, K. M.; Riva, C.; Guzman, R. Effect of Acute Ozone Exposure on Locomotor Behavior and Striatal Function. *Pharmacol., Biochem. Behav.* **2003**, *74*, 891−900.

(9) Medintz, I. L.; Clapp, A. R.; Brunel, F. M.; Tiefenbrunn, T.; Uyeda, H. T.; Chang, E. L.; Deschamps, J. R.; Dawson, P. E.; Mattoussi, H. Proteolytic Activity Monitored by Fluorescence Resonance Energy Transfer Through Quantum-Dot−Peptide Conjugates. *Nat. Mater.* **2006**, *5* (7), 581−589.

(10) Liu, S.; Zhang, X.; Yu, Y.; Zou, G. A Monochromatic Electrochemiluminescence Sensing Strategy for Dopamine with Dual-Stabilizers-Capped CdSe Quantum Dots as Emitters. *Anal. Chem.* **2014**, *86*, 2784−2788.

(11) Chou, K.; Meng, H.; Cen, Y.; Li, L.; Chen, J.-Y. Dopamine−Quantum Dot Conjugate: A New Kind of Photosensitizers for Photodynamic Therapy of Cancers. *J. Nanopart. Res.* **2013**, *15*, 1348.

(12) Liu, J.; Bao, C.; Zhong, X.; Zhao, C.; Zhu, L. Highly Selective Detection of Glutathione Using a Quantum-Dot-Based OFF−ON Fluorescent Probe. *Chem. Commun.* **2010**, *46*, 2971−2973.

(13) Yuan, J.; Guo, W.; Wang, E. Utilizing a CdTe Quantum Dots−Enzyme Hybrid System for the Determination of Both Phenolic Compounds and Hydrogen Peroxide. *Anal. Chem.* **2008**, *80*, 1141−1145.

(14) Gill, R.; Freeman, R.; Xu, J.-P.; Willner, I.; Winograd, S.; Shweky, I.; Banin, U. Probing Biocatalytic Transformations with CdSe−ZnS QDs. *J. Am. Chem. Soc.* **2006**, *128*, 15376−15377.

(15) Medintz, I. L.; Stewart, M. H.; Trammell, S. A.; Susumu, K.; Delehanty, J. B.; Mei, B. C.; Melinger, J. S.; Canosa, J. B. B.; Dawson, P. E.; Mattoussi, H. Quantum-Dot/Dopamine Bioconjugates Function as Redox Coupled Assemblies for in Vitro and Intracellular pH Sensing. *Nat. Mater.* **2010**, *9*, 676−684.

(16) Ji, X.; Palui, G.; Avellini, T.; Na, H. B.; Yi, C.; Knappenberger, K.; Mattoussi, H. On the pH-Dependent Quenching of Quantum Dot Photoluminescence by Redox Active Dopamine. *J. Am. Chem. Soc.* **2012**, *134*, 6006−6017.

(17) Ma, W.; Qin, L. X.; Liu, F. T.; Gu, Z.; Wang, J.; Pan, Z. G.; James, T. D.; Long, Y.-T. Ubiquinone-Quantum Dot Bioconjugates for in Vitro and Intracellular Complex I Sensing. *Sci. Rep.* **2013**, *3*, 1537−1544.

(18) Qin, L. X.; Ma, W.; Li, D. W.; Li, Y.; Chen, X.; Kraatz, H.-B.; James, T. D.; Long, Y.-T. Coenzyme Q Functionalized CdTe/ZnS Quantum Dots for Reactive Oxygen Species (ROS) Imaging. *Chem.—Eur. J.* **2011**, *17*, 5262−5271.

(19) Li, D.-W.; Qin, L. X.; Li, Y.; Nia, R. P.; Long, Y.-T.; Chen, H.-Y. CdSe/ZnS Quantum Dot−Cytochrome c Bioconjugates for Selective Intracellular $O_2^{\bullet-}$ Sensing. *Chem. Commun.* **2011**, *47*, 8539−8541.

(20) Rogach, A. L.; Franzl, T.; Klar, T. A.; Feldmann, J.; Gaponik, N.; Lesnyak, V.; Shavel, A.; Eychmüller, A.; Rakovich, Y. P.; Donegan, J. F. Aqueous Synthesis of Thiol-Capped CdTe Nanocrystals: State-of-the-Art. *J. Phys. Chem. C* **2007**, *111* (40), 14628−14637.

(21) Aldeek, F.; Hawkins, D.; Palomo, V.; Safi, M.; Palui, G.; Dawson, P. E.; Alabugin, I.; Mattoussi, H. UV and Sunlight Driven Photoligation of Quantum Dots: Understanding the Photochemical Transformation of the Ligands. *J. Am. Chem. Soc.* **2015**, *137*, 2704−2714.

(22) Grabolle, M.; Spieles, M.; Lesnyak, V.; Gaponik, N.; Eychmüller, A.; Resch-Genger, U. Determination of the Fluorescence Quantum Yield of Quantum Dots: Suitable Procedures and Achievable Uncertainties. *Anal. Chem.* **2009**, *81* (15), 6285−6294.

(23) Ma, W.; Liu, H.-T.; He, X.- P.; Zang, Y.; Li, J.; Chen, G.-R.; Tian, H.; Long, Y.-T. Target-Specific Imaging of Transmembrane Receptors Using Quinonyl Glycosides Functionalized Quantum Dots. *Anal. Chem.* **2014**, *86*, 5502−5507.

(24) Winter, E.; Codognoto, L.; Rath, S. Electrochemical Behavior of Dopamine in the Presence of Citrate: Reaction Mechanism. *Electrochim. Acta* **2006**, *51*, 1282−1288.

(25) Barreto, W. J.; Ponzoni, S.; Sassi, P. A Raman and UV−Vis Study of Catecholamines Oxidized with Mn(III). *Spectrochim. Acta, Part A* **1999**, *55*, 65−72.

(26) Ma, W.; Li, D.-W.; Sutherland, T. C.; Li, Y.; Long, Y.-T.; Chen, H.-Y. Reversible Redox of NADH and NAD^+ at a Hybrid Lipid Bilayer Membrane Using Ubiquinone. *J. Am. Chem. Soc.* **2011**, *133*, 12366−12369.

(27) Zhang, Y. Z.; Zhou, B.; Zhang, X.-P.; Huang, P.; Li, C.-H.; Liu, Y. Interaction of Malachite Green with Bovine Serum Albumin: Determination of the Binding Mechanism and Binding Site by Spectroscopic Methods. *J. Hazard. Mater.* **2009**, *163*, 1345−1352.

(28) Zhang, Y. Z.; Zhou, B.; Liu, Y.-X.; Zhou, C.-X.; Ding, X.-L.; Liu, Y. Fluorescence Study on the Interaction of Bovine Serum Albumin with p-Aminoazobenzene. *J. Fluoresc.* **2008**, *18*, 109−118.

(29) Long, Y.-T.; Kong, C.; Li, D.-W.; Li, Y.; Chowdhury, S.; Tian, H. Ultrasensitive Determination of Cysteine Based on the Photocurrent of Nafion-Functionalized CdS−MV Quantum Dots on an ITO Electrode. *Small* **2011**, *12*, 1624−1628.

(30) Ma, Y.; Liu, S.; Yang, H.; Wu, Y.; Yang, C.; Liu, X.; Zhao, Q.; Wu, H.; Liang, J.; Li, F.; Huang, W. Water-Soluble Phosphorescent Iridium(III) Complexes as Multicolor Probes for Imaging of Homocysteine and Cysteine in Living Cells. *J. Mater. Chem.* **2011**, *21*, 18974−18982.

(31) Schnürch, A. B.; Hornof, M.; Zoidl, T. Thiolated Polymers—Thiomers: Synthesis and in Vitro Evaluation of Chitosan−2-Iminothiolane Conjugates. *Int. J. Pharm.* **2003**, *260*, 229−237.

DOI: 10.1021/acsami.5b03044
ACS Appl. Mater. Interfaces 2015, 7, 14352−14358

(32) Ellman, G. L. Tissue Sulfhydryl Groups. *Arch. Biochem. Biophys.* **1959**, *82*, 70−77.
(33) Clarke, S. J.; Hollmann, C. A.; Zhang, Z.; Suffern, D.; Bradforth, S. E.; Dimitrijevic, N. M.; Minarik, W. G.; Nadeau, J. L. Photophysics of Dopamine-modified Quantum Qots and Effects on Biological Systems. *Nat. Mater.* **2006**, *5* (5), 409−417.
(34) Elphick, G. F.; Querbes, W.; Jordan, J. A.; Gee, G. V.; Eash, S.; Manley, K.; Dugan, A.; Stanifer, M.; Bhatnagar, A.; Kroeze, W. K.; Roth, L.; Atwood, W. J. The Human Polyomavirus, JCV, Uses Serotonin Receptors to Infect Cells. *Science* **2004**, *306*, 1380−1383.
(35) Ruan, G.; Agrawal, A.; Marcus, A. I.; Nie, S. Imaging and Tracking of Tat Peptide-Conjugated Quantum Dots in Living Cells: New Insights into Nanoparticle Uptake, Intracellular Transport, and Vesicle Shedding. *J. Am. Chem. Soc.* **2007**, *129* (47), 14759−14766.
(36) Zhu, X.; Hu, J.; Zhao, Z.; Sun, M.; Chi, X.; Wang, X.; Gao, J. Kinetic and Sensitive Analysis of Tyrosinase Activity Using Electron Transfer Complexes: in Vitro and Intracellular Study. *Small* **2015**, *11* (7), 862−870.
(37) Jaiswal, J. K.; Mattoussi, H.; Mauro, J. M.; Simon, S. M. Long-term Multiple Color Imaging of Live Cells Using Quantum Dot Bioconjugates. *Nat. Biotechnol.* **2003**, *21* (1), 47−51.

DOI: 10.1021/acsami.5b03044
ACS Appl. Mater. Interfaces 2015, 7, 14352−14358